Volume 10 Number 18 1982 Nucleic Acids Research

Structural transitions in viroid-like RNAs associated with cadang-cadang disease, velvet tobacco mottle virus, and *Solanum nodiflorum* mottle virus

John W.Randles*, Gerhard Steger and Detlev Riesner

Institut für Physikalische Biologie, Universität Düsseldorf, Universitätsstrasse 1, D-4000 Düsseldorf 1, FRG

Received 31 August 1982; Accepted 6 September 1982

ABSTRACT

The conformational transitions of viroid-like RNAs associated with cadang-cadang disease, velvet tobacco mottle virus, and solanum nodiflorum mottle virus were studied by melting analysis and fast temperature jump technique in 1 mM sodium-cacodylate, 10 mM NaCl, 0.1 mM EDTA, pH 6.8. The 4 circular RNAs of cadang-cadang show a highly cooperative transition between 45 and 49°C, respectively, and a second transition of less hypochromicity at about 10°C higher temperatures. The data are interpreted quantitatively on the basis of the sequences and secondary structure models. A very similar scheme for the structure and structural transitions as derived earlier for other viroids applies to the cadang-cadang RNAs. In the main transition the total native secondary structure is disrupted and a stable hairpin consisting of 9 base pairs is newly formed which dissociates in the second transition. The thermal denaturation of the circular RNAs from the viruses mentioned above is clearly distinct from viroid RNA in respect to stability and cooperativity. The results on cadang-cadang RNA are discussed in the light of recent hypotheses about the interference of viroids with the splicing process of the host cell.

INTRODUCTION

Cadang-cadang disease of coconut has a putative viroid etiology /1,2/ based on the viroid-like structural properties /3,4/ of one of the disease-associated ccRNAs /5/. However, it differs from other diseases known to be caused by viroids in that two unique, but related, ccRNA species (ccRNA1 and ccRNA2) are associated with the disease /1,6/, and each of these show variants /7/ which differ in electrophoretic mobility and molecular weight. Here the fast /7/ electrophoretic form is termed "small", the slow /7/ form is termed "large". Data on the infectivities of these RNAs are incomplete /7,8/ as the relative infectivities of the different forms are still being assessed.

A new class of low molecular weight, circular, single-stranded, viroid-like RNA molecules has recently been discovered, encapsidated in virus particles. The first examples of this were in velvet tobacco mottle and solanum

0305-1048/82/1018-5569$ 2.00/0

nodiflorum mottle viruses (VTMoV /9/, SNMV /9/) /10-12/. Each virus contains one viroid-like species, these two species differing slightly from each other in length and nucleotide sequence /12/. They differ from viroids because they depend upon the high molecular weight viral RNA component for replication /13/. Despite their inability to replicate autonomously, their structure implies a relationship to viroids, and it seems possible that they may exert a regulatory function on virus replication as they are essential for the replication of the other viral RNA components. Thus they may have a function similar to that proposed for viroids but this may be exerted on virus synthesis rather than on host plant metabolism /3/.

Studies with viroids have shown that they share a number of structural properties. They are circular; they have conserved nucleotide sequences /14, 15,16/; and they have characteristic thermal denaturation properties such as cooperative melting and the production of stable intermediates resulting from the formation of new hairpin structures after the first cooperative melt /17,18/ of the rod-shaped native structure.

The question of the structural similarity between the putative cadang-cadang viroid in all its forms, the viroid-like molecules of VTMoV and SNMV, and the previously studied viroids now arises. Since molecular function is determined by structure, a comparison of molecular structures may show a correlation between particular structural features and biological function.

Symons and his coworkers /19,20/ have determined the primary sequences of a representative group of the cadang-cadang RNAs and the viroid-like RNAs of VTMoV and SNMV. Their data (cf. Fig. 6) indicate that a nucleotide sequence almost identical to that conserved in the other viroids is found in the cadang-cadang associated RNAs; that ccRNA1 is a monomer with either one (ccRNA1-small) or two copies (ccRNA1-large) of one small sequence; that ccRNA2 is a dimer of these molecules (ccRNA2-small and ccRNA2-large). In contrast, the VTMoV and SNMV RNAs have no sequences typical of those which are conserved in viroids. Our studies have centred on the dynamic secondary structural features of this group of RNAs with particular emphasis on a comparison with the principles previously shown to apply to the viroids /17,18,21,33/. Here we describe the results of thermodynamic studies on melting behaviour, the accurrence of structural intermediates during thermal denaturation, and present a model of the secondary structural features of the cadang-cadang molecules consistent with our experimental observations.

MATERIALS AND METHODS

Preparation of viroid-like RNA

The ccRNAs were isolated from leaves of diseased coconut palms. Extracts of sap in 0.1 M Na_2SO_3 were strained, clarified, and mixed with polyethyleneglycol (PEG) 6000 to 5% /1/. Nucleic acids in the PEG-insoluble fraction were extracted by one of several methods based on phenol-sodium dodecyl sulphate-chloroform extraction, and a 2 M salt fractionation step /1,7,22/. Nucleic acids were precipitated in ethanol, dried, and then dissolved in electrophoresis buffer.

Further purification was achieved by polyacrylamide gel electrophoresis under non-denaturing and denaturing conditions /22/. ccRNA1 and ccRNA2 /1/ were first separated on 5% slab gels containing Tris-borate-EDTA (TBE) buffer /23/. The bands were stained with toluidine blue, cut out, and the gel pieces were laid directly on top of TBE-buffered 5% slab gels containing 8 M urea. The circular (c) and linear (l) forms of ccRNA1 and ccRNA2 were separated during electrophoresis under these denaturing conditions, and were again detected by staining. The RNA in each of the bands was finally recovered by electrophoresis of the RNA from an excised gel piece into a 3.3% polyacrylamide preparative gel slab, and elution of the RNA from the bottom of the gel, using the preparative adaptor for the Biorad Model 220 gel apparatus /7/. RNA was precipitated from the appropriate fractions with ethanol, in the presence of 0.1 M sodium acetate.

The RNA components of VTMoV and SNMV were extracted by incubating purified virus /10/ with pronase-sodium acetate-sodium dodecyl sulphate at 37°C for 16 hr, followed by extraction with phenol-cresol /1,23/. Nucleic acids were precipitated with ethanol. All RNA preparation were dried and stored at -20°C except during transport.

Before physical studies were done circular molecules of ccRNA1 and ccRNA2 were separated from small amounts of linear molecules formed during storage. Preparations were dissolved in 50% glycerol and 0.5 M TBE and subjected to electrophoresis at 40°C on 3.3% polyacrylamide gels containing 8 M urea and TBE. The circular RNAs of VTMoV and SNMV were separated from other viral RNA component by electrophoresis on 5% polyacrylamide-urea gels.

Bands were detected by staining in aqueous toluidine blue (c. 0.01%), excised, and blended with 1 ml of 2 M sodium acetate buffer, pH 6.9 in an Ultraturrax. Watersaturated phenol (0.25 ml) was added, and the slurry was shaken for 16 hr at 4°C. After centrifugation at 15000 g for 15 min, the supernatant was removed and the gel fragments were washed for at least 30 min

for three more times with 1 ml of water and 1 ml phenol, recovering the aqueous phase after each wash. RNA was recovered by precipitation with three volumes of ethanol. The RNA pellet was washed with ethanol, dried, and dissolved in 200 µl of 0.1 NaCl. One half-volume of sterile 1% cetyl trimethylammonium bromide was added /14/ and the resulting RNA precipitate was washed with 0.1 M sodium acetate in 75% ethanol and dried.

The RNA was dissolved in standard buffer (10 mM NaCl, 1 mM sodium cacodylate, and 0.1 mM EDTA) pH 6.8 /25/ and dialysed for at least 24 hr against standard buffer. Preparations were analyzed for purity on polyacrylamide-urea gels, and stored at -20°C.

Equilibrium thermal denaturation studies

RNA samples (40 µl) were adjusted to a concentration of about 10 µg/ml (A_{260} = 0.25) in standard buffer saturated with He, and loaded into a flow cuvette of 1 cm pathlength (HELLMA, Müllheim, GFR) /26/. The cuvette was sealed with spectral grade paraffin oil (Uvasol, Merck) which had been previously autoclaved over standard buffer. The cuvette was placed in a cell holder, in which the temperature was controlled by a Julabo thermostat F 20 HC (Julabo, Juchheim, GFR). Temperature was measured with a NTC-resistor placed in the water lead adjacent to the cuvette holder. The optical measurements were done in a dual wavelength spectrophotometer (Sigma ZWS 11, Biochem, München, GFR) in which the two light beams are guided with a quartz fiber directly to the front of the cuvette. The photomultiplier, which is about 3 cm behind the cuvette, was held at 30°C. The drift was less than 0.5 mA/hr. The absorption values (260 and 280 nm) and the temperature values were passed through a 12 bit A/D converter (Technosystem , Heidelberg, GFR) to an Apple II computer at a rate of 20 points/°C . The thermostat was programmed by the computer with a 12 bit D/A converter (Technosystem , Heidelberg, GFR) to increase temperature at a rate of 0.3°C/min. Smaller temperature increases gave the same results. Thermal denaturation profiles were fitted and differentiated by linear interpolation including 9 to 19 data points depending on the width of the transition. G+C content was determined according to Fresco et al. /27/ and Coutts /28/. After normalizing the denaturation curves to 1 A_{260} at 20°C they were plotted on a x-y recorder.

Fast kinetic measurements

Fast kinetic studies were carried out in a modified version of an Eigen-De Maeyer temperature jump apparatus as described elsewhere /29/. A commercially available cell was modified for use with low volume samples of 80 µl by forming a gel of 5% agarose (deionized, sterile, high gelling temperature agarose, Sigma Chemical Co.) between the electrodes, and placing the sample

in a hole of small bore cut from one window to the other /30/. The heating time under the buffer conditions used was approximately 30 µs, and the jump was 3°C for a 20 kV discharge. Evaluation was carried out by an analog simulation technique similar to that described earlier /31/.

Calculation of thermodynamic parameters

The values of ΔH and ΔS for base pair formation and loop formation were very close to those used earlier /17/, but were slightly modified, on the basis of newer results on double-stranded viral RNA /25/. The whole set of parameters will be given elsewhere (Steger, Gross, Randles, Sänger, and Riesner, manuscript in preparation). The nucleation parameter σ for intermolecular base pairing was assumed 10^{-3}.

RESULTS

Equilibrium thermal denaturation

1) Cadang-cadang RNA

i) Two characteristic transitions

Fig. 1 shows several examples of denaturation curves of different forms of ccRNA, all measured in standard buffer. For a closer comparison under absolutely identical buffer conditions, mixtures of two different RNA species were investigated in some cases. As mentioned under "Methods" the absorption at 260 nm and 280 nm was recorded in the same heating procedure and the differentiated melting curve was calculated from the values at 260 nm.

The denaturation of ccRNA1, small form and large form, shows the characteristic behaviour of viroid melting, i.e. a denaturation temperature (T_{M1}) around 50°C in standard buffer and a very narrow transition range. These features as mentioned previously /2/ are similar to those found in potato spindle tuber-, citrus exocortis-, and chrysanthemum stunt viroid /21/. A second transition (T_{M2}) of much lower hypochromicity is clearly detectable at temperatures about 10°C higher than the main transition. In the viroids from potato, citrus and chrysanthemum, however, similar transitions had not been resolved in the equilibrium denaturation, but were followed by kinetic techniques /18/.

In Table 1 the values of T_{M1}, the half width $\Delta T_{1/2}$ and T_{M2} together with several other parameters are given for cadang-cadang RNA, VTMoV-RNA, and SNMV-RNA.

ii) Dependence upon size, source, and circularity

When the small and the large forms of ccRNA1 were mixed in about equal amounts the denaturation curve of the mixture showed a half width of 1.3°C which is the average between the value of the small (1.4°C) and the large

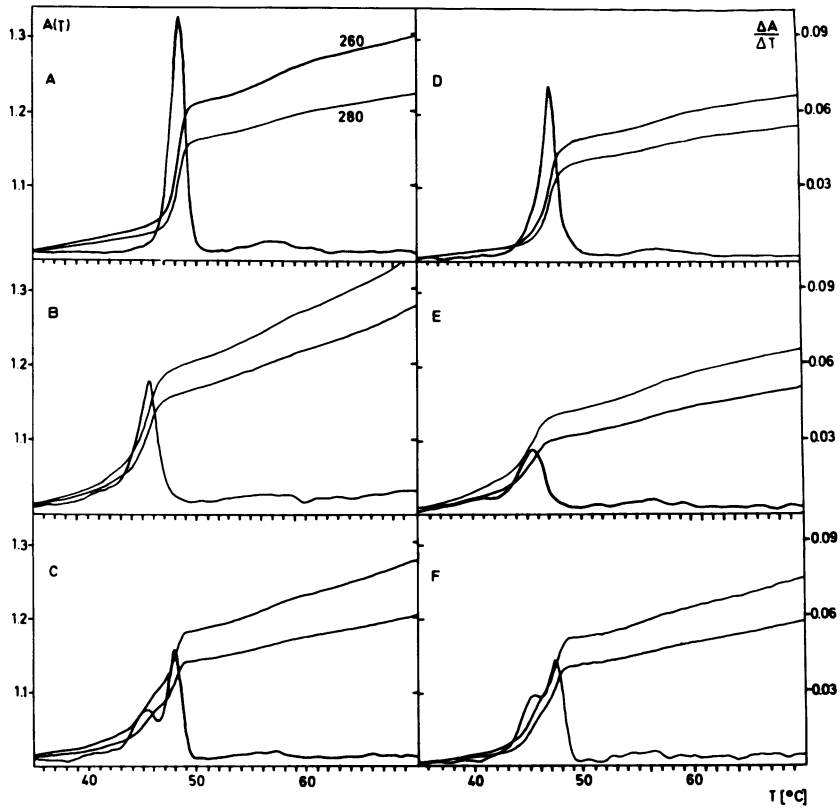

Fig. 1: Denaturation curves of different forms of ccRNA in standard buffer. Integrated curves A(T) were measured at 260 and 280 nm, differentiated curves $\Delta A/\Delta T$ were calculated at 260 nm. A: circular ccRNA1-small; B: linear ccRNA1-small; C: mixture of circular and linear ccRNA1-small; D: circular ccRNA2-large; E: linear ccRNA2-small; F: mixture of circular ccRNA1-large and ccRNA2-large.

form (1.2°C). Thus, the T_{M1}-values of both forms are identical within the limits of errors. Small differences could be determined much more accurately in experiments on mixtures than by comparison of the T_{M1}-values from separate runs using single samples.

The T_{M1} of ccRNA2 is about 2°C lower than ccRNA1, whereas the T_{M2}-values were not significantly different from those of ccRNA1. Again, the differences in T_{M1} were obtained most accurately from experiments on mixtures of both species, in which two transitions could clearly be resolved (cf. Fig. 1F). The half width of the main transition in both forms of circular ccRNA2 is significantly broader than in ccRNA1.

Table 1: Comparative parameters of thermal denaturation of the viroid-like RNAs.

		ccRNA1				ccRNA2			CIRCULAR RNA FROM	
		SMALL		LARGE		SMALL		LARGE		
		CIRCULAR	LINEAR	CIRCULAR	LINEAR	CIRCULAR	LINEAR	CIRCULAR	VTMoV	SMNV
transition 1	T_{M1} [°C]	49.1	45.6	49.4	45.2	46.7	45.7	47.1	38.1	38.2
	ΔT_M [°C]	2.7		2.5		<0.5			<0.5	
		<0.2				<0.5				
				2.3						
		1.7								
	$\Delta T_{1/2}$ [°C]	1.4	2.9	1.2	2.8	2.4	2.7	1.6		
	Hy [%]	15.0	10.5	16.5	15.0	12.0	8.5	14.5	9.0	10.0
	f_{GC} [%]	70.0	73.5	72.5	73.0	73.0	72.5	74.0		
2	T_{M2} [°C]	57.5	56.5	57.5	55.0	57.0	56.0	56.0		
	Hy [%]	2.3		2.0	1.5	1.9	1.5	<1.8		

Midpoint temperature (T_M) and differences in T_M (ΔT_M) were evaluated from independent measurements, i.e. from samples of one RNA only or from a mixture of two RNAs, respectively. $\Delta T_{1/2}$: half width; Hy: hypochromicity; f_{GC}: content of G:C base pairs dissociating in the corresponding transition. Standard error of T_M is ±0.5°C, of ΔT_M ±0.3°C, of $\Delta T_{1/2}$ ±0.1°C, and of Hy ±1.0%.

The circular forms of cadang-cadang RNA have been compared also to the linear forms. In ccRNA1 the main transition in the linear forms is about 2.5°C lower than in the corresponding circular forms and the transition is significantly broader. In ccRNA2, circular and linear forms denature without significant differences. It should be pointed out that the linear forms were separated from the circular forms in the original plant extracts (see Material and Methods). These linear forms may differ in their site of cleavage from those which are generated from circles after long preparation procedures or long storage times and it is not known, whether these sites of cleavage are specific, partially specific, or random.

The melting characteristics of the circular ccRNA1 are independent of source. The same melting profiles were observed for ccRNA1 when obtained from different palms. Furthermore both small and large forms either from the same or different palms, gave the same profiles.

iii) Dependence upon ionic strength

The denaturation profiles of ccRNA1-large have been followed in ionic strengths of 0.01 M, 0.1 M, and 1.0 M. The result is shown in Fig. 2. Evidently, the high cooperativity of the main transition is expressed only in low ionic strength and is gradually lost with increasing ionic strength. In 1 M ionic strength three fairly broad and not well resolved transitions are detectable.

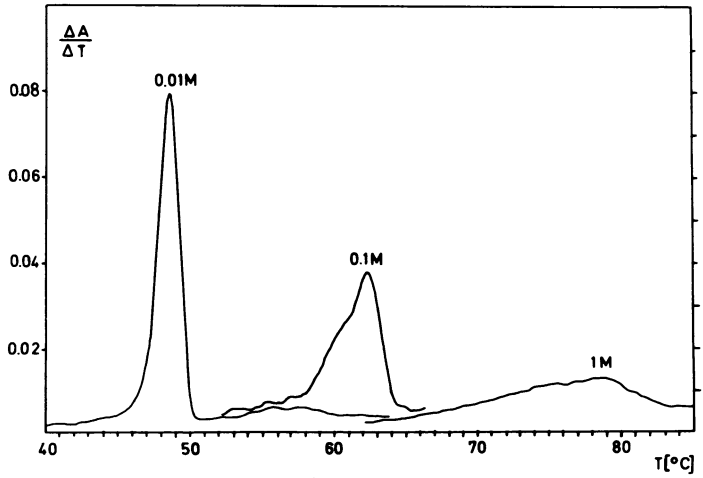

Fig. 2: Ionic strength dependence of the denaturation curves of ccRNA1-large

2) Circular RNA from VTMoV and SNMV

The denaturation curves in Fig. 3 show a cooperative transition for VTMoV- and SNMV-RNA about 10°C lower than ccRNA1. If the T_M-value of VTMoV-RNA reported recently by Gould /11/ is extrapolated to the buffer conditions used in this study, fair agreement is found. The present measurement on the mixture of RNA from VTMoV and SNMV, however, results in nearly identical T_M-values for both RNA (cf. Table 1) in contrast to a previous report /11,12/. The hypochromicity of the cooperative transition is lower than in cadang-cadang-RNA (cf. Table 1) and more melting occurred below and above this transition than with ccRNA1. The hypochromicity, however, cannot be evaluated quantitatively because the samples of circular RNA from VTMoV and SNMV may not be as pure as those from cadang-cadang. For example VTMoV-RNA was contaminated to a level of 10-20% with faster sedimenting material as assessed by analysis in the analytical ultracentrifuge /32/.

Kinetic Investigations

Temperature jump experiments have been carried out to obtain quantitative information of the second transition (T_{M2}). In kinetic studies a denaturation process is characterized not only by an overall absorption change but also by its characteristic time course. Therefore, a specific denatura-

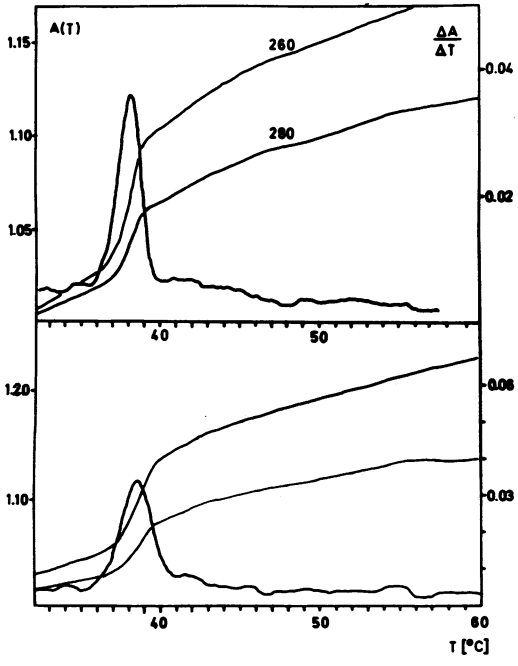

Fig. 3: Denaturation curves at 260 and 280 nm, and differentiated curve at 260 nm of circular RNA from VTMoV (upper) and SNMV (lower) in standard buffer.

tion process may be well differentiated from the unspecific stacking - unstacking equilibrium of single stranded RNA which leads to the continous increase in absorption above the main transition.

The kinetic measurements were carried out on ccRNA1-large in standard buffer. Fig. 4 shows a typical oscilloscope trace. A single relaxation process in the time range of several hundred microseconds is observed. The relaxation amplitudes and relaxation times τ were followed systematically over the temperature range of the second transition. The amplitudes yielded the differentiated melting curve of the corresponding transition as shown in Fig. 5 (bottom). From this the equilibrium constant K(T) was evaluated.

With $K = k_R/k_D$, and $1/\tau = k_R + k_D$ both rate constants (k_R for recombination, k_D for dissociation) were obtained as a function of the temperature. The values of K, k_R, k_D, and $1/\tau$ are presented in Fig. 5 (top) in form of a van't Hoff- and an Arrheniusplot, respectively. From the slopes of the interpolated straight lines the reaction- and activation-enthalpies, respectively, were evaluated. Although the points show considerable scatter the interpolation shows a unique set of data which is consistent with both, the temperature dependence of the relaxation times, and the relaxation amplitudes.

The results from further evaluations are listed in Table 2. The T_{M2}-value was extrapolated to 1 M ionic strengtn for better comparison with model calculations which have to be carried out under these conditions. In standard buffer T_{M2} was some degrees higher in the kinetic studies than in the equilibrium melting curve (cf. Table 1). This may be explained in several ways; degassing the solution in the micro-T-jump cell may lead to a slight increase

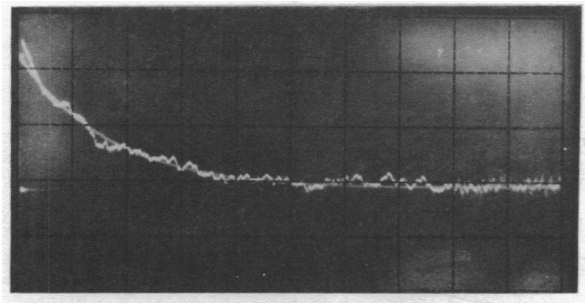

Fig. 4: Oscillogram of the temperature jump relaxation curve in the second transition. RNA concentration was about 1 A_{260}/optical pathlength of 7 mm; the jump was recorded at 280 nm. Oscilloscope settings: 500 µs/div time scale; 25 mV/div sensitivity. Total signal was 10 V; noise filter 100 µs; final temperature 65°C; temperature jump 3°C. The simulated exponential with τ^{-1} = 1700 s^{-1} is superimposed.

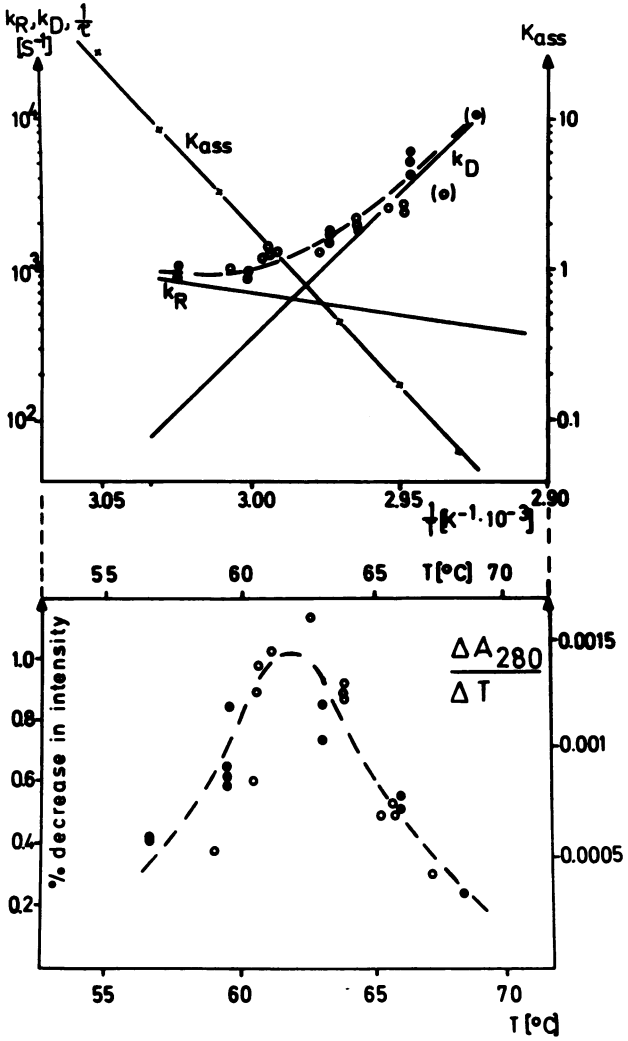

Fig. 5: van't Hoff and Arrhenius plot (upper figure) and temperature dependence of the relaxation amplitudes (lower figure) of the second transition of ccRNA1-large in standard buffer. Open and full circles belong to two different sets of experiments.

in ion concentration; or the temperature in the solution may be lower than in the electrode of the cell where the temperature is measured. The slight shift in temperature does not, however, affect the conclusion given below. At the optimal temperature the amplitudes have been measured at 260 and 280 nm in order to evaluate from their ratio at the two wavelengths the G:C content of the dissociating basepairs. The G:C content and the reaction enthalpy allows the number of basepairs involved to be calculated. Further information on the structure involved in the transition comes from the absolute value of the re-

combination rate constant k_R. As described by Henco et al. /18/ the size of the loop which is formed by the basepairs can be estimated from the rate constant. In circular viroids formation of a double helical stretch leads to the appearance of a loop on either side, and it is the small loop which determines the magnitude of the rate constant.

DISCUSSION

The thermodynamic investigations of cadang-cadang-RNA and the circular RNA of VTMoV and SNMV have shown which properties of these viroid-like RNAs fit into the general picture of the structure and structural transitions of other viroids /17,18,21,33/ and which are clearly different.

The sequence of ccRNA as determined by Haseloff et al. /19/ can be arranged for all 4 forms of cadang-cadang-RNA in a secondary structure (Fig.6) with the form of a linear arrangement of short double helices and small internal loops as proposed in a general scheme for the other viroids. The similarity in the secondary structure between ccRNA and the other viroids was not to expect a priori because the sequence homology to other viroids /14,15,16/ is restricted to a small boxed region shown in Fig. 6. The structural principle holds also for the secondary structure of the circular RNA from VTMoV and SNMV as derived from the sequences of Haseloff and Symons (not shown), but a significant sequence homology with the other viroids has not been found /20/.

The melting curves in standard buffer show that T_{M1}-values, cooperativity and hypochromicity of ccRNA1 (small and large form) are very similar to those of other viroids. Consequently, the thermodynamic features are a strong experimental support for the presence of the structure as proposed in Fig. 6 because the same arguments hold for ccRNA1 as for the other viroids /17,18, 21,33/. The cooperativity seems to be expressed even more clearly because $\Delta H_{van't\ Hoff}$ is 2950 kJ/Mol for the large form and 2500 kJ/Mol for the small form. According to the denaturation mechanism (see below) these values correspond to nearly 100% cooperativity whereas only 80-90% cooperativity was found in other viroids /21/. Further discussion will concentrate on those features which are more specific for cadang-cadang-RNA and RNA from VTMoV and SNMV.

1) Circular RNA from VTMoV and SNMV is clearly distinct from viroid RNA

Whereas the T_{M1}-values of all the viroids studied so far /18,21/ and of ccRNA1 are within a range of 3°C, the T_{M1}-values of the RNA from VTMoV and SNMV are 10°C lower than the characteristic range. The cooperativity is also markedly lower. The hydrodynamic properties (accompanying paper /32/) show that the flexibility of these RNAs is higher than that of the other viroids.

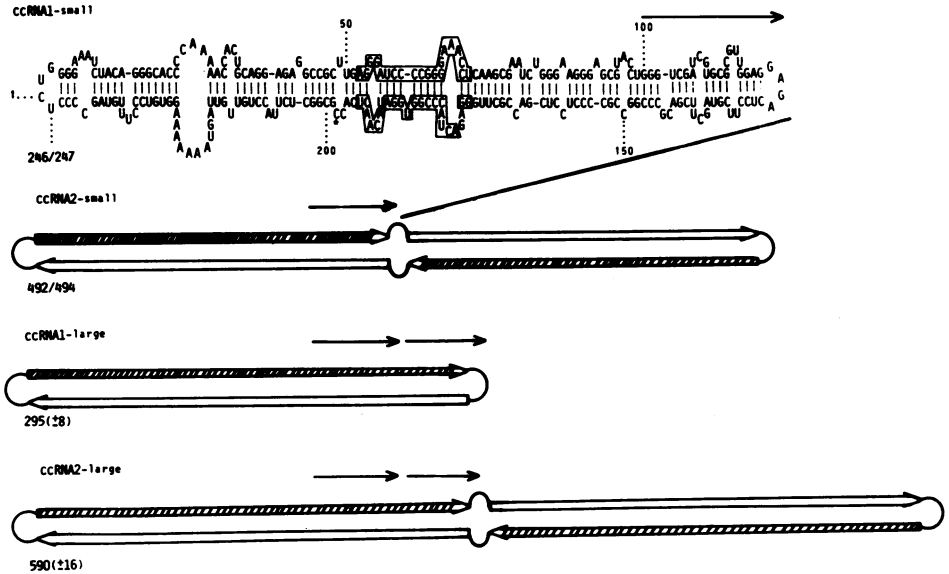

Fig. 6: Nucleotide sequences and secondary structures of ccRNAs according to Haseloff, Mohamed and Symons /19/. ccRNA1-small used in this work (isolate Ligao 620c) is a mixture of 40% with nucleotide C 198 (marked with the star) and 60% without C 198. The sequences in the boxed regions are identical to those of other viroids /14,15,16/. The arrow at the right side of ccRNA1-small indicates that this segment (upper and lower part of the strand) is duplicated in ccRNA1-large. The length of the duplicated segemnt in ccRNA1-large however, varies between different isolates sequenced from 41 to 55 nucleotides. Because ccRNA-large used in this work (isolate 71) has not been sequenced so far one has to assume an uncertainty in the length of the arrow of ±4 nucleotides. ccRNA2 is an exact duplication of ccRNA1 as indicated by the solid line and the open and full arrows of the complementary regions. ccRNA2 can be arranged also in a form in which the internal middle loop would form the two hairpin end loops and vice versa. This form is favoured by Haseloff et al. /19/ on the basis of digestion patterns but cannot be favoured for thermodynamic or hydrodynamic reasons (cf. accompanying paper /32/).

Therefore, from the dynamic point of view, it can be stated that the circular RNA from VTMoV and SNMV do not possess features typical of viroids.

2) Formation of one stable hairpin during the denaturation of cadang-cadang-RNA1

The thermodynamic and kinetic properties of the second transition can be described from the fast kinetic investigations. A systematic search for the most stable hairpin in the sequence led to the one shown in Table 2. The parameters calculated for this structure agree very well with those measured in the second transition. Therefore, it is safe to conclude that it is this

Table 2: Properties of the stable hairpin of ccRNA1-large. Calculated values (the) refer to the nucleotide sequence, experimental values (obs) are taken from T-jump-measurements. The observed T_M-value is extrapolated from experimental conditions to 1 M ionic strength with a value of $dT_M/d \log c_{Na+}$ of 16°C.

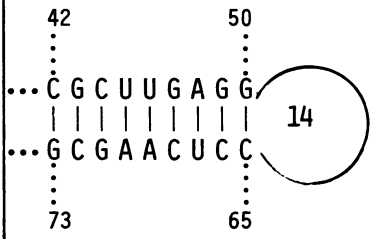

	the	obs
T_m |°C|	85	87 ±2
% G:C	67	71 ±7
loop size	14	20 ±10
base pairs	9	9 ±2
reaction enthalpy ΔH |kJ/mol|	-414	-400 ±60
activation enthalpy of dissociation ΔE |kJ/mol|	--	350 ±50

hairpin which dissociates in the second transition. A hairpin with a very similar sequence in the homologous position has been found in PSTV, CEV, and CSV /17,18,33/. However, only with ccRNA was it possible to determine thermodynamic properties with fairly high accuracy because only here was the transition well resolved, i.e. not superimposed on the transitions of other stable hairpins as with the other viroids. The appearance of this stable hairpin - termed hairpin I in the other viroids - bears a striking similarity to the viroids studied and supports the "viroid-likeness" of cadang-cadang, whereas the absence of the other stable hairpins shows a clear difference between cadang-cadang and the other viroids. As previously discussed in detail /17,18/, the stable hairpin is not part of the native structure but is newly formed during the main transition. The proposed denaturation mechanism is shown in Fig. 7.

3) Electrostatic contribution to the cooperativity

The denaturation process of ccRNA1 is highly cooperative in low ionic strength but loses its cooperativity with increasing ionic strength (Fig. 2). This behaviour has not been found in other viroids /21/. In a forthcoming paper we will describe the theoretical simulation of the denaturation process of different viroids and ccRNA. Here we will discuss only qualitatively that the observed effect in ccRNA1 may be explained partly by the particular properties of the final double helix at the right side. This double helix is

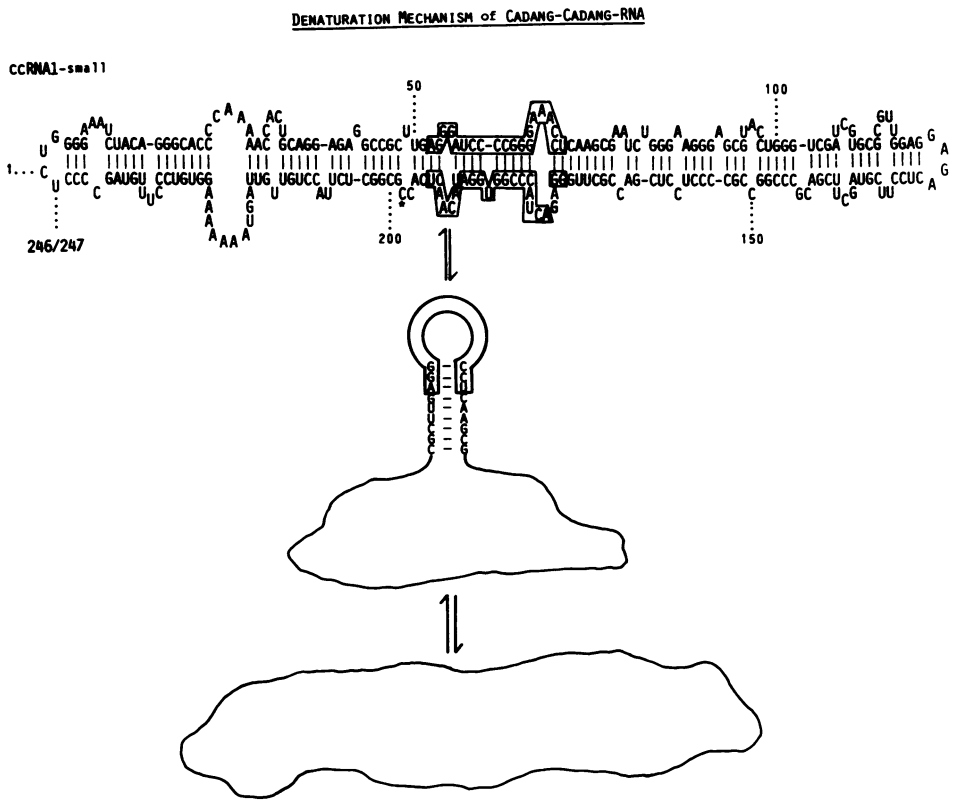

Fig. 7: Denaturation mechanism of ccRNA1 (here shown with the established sequence of ccRNA1-small). The transition from the native structure to the hairpin structure corresponds to the main transition of melting curves, and the transition to the unpaired circle with the high temperature transition. For the boxed region confer Fig. 6.

high in GC and the adjacent hairpin loop contains only 4 bases. According to the results with other small hairpins /28/, the stability of this helix is expected to depend only slightly upon the ionic strength, i.e. less than the rest of the viroid molecule. Therefore, it may be possible that the final helix is more stable than the rest of the molecule at low ionic strength and less stable at high ionic strength. This would lead to an increase in stability and cooperativity of the main transition only at low ionic strength as it was observed in the experiment.

In ccRNA2 which is an exact duplicate of ccRNA1, the boundary between both ccRNA1-like halves is formed by an internal loop with 8 bases. Therefore, each of the halves is missing one hairpin loop and the particular influence

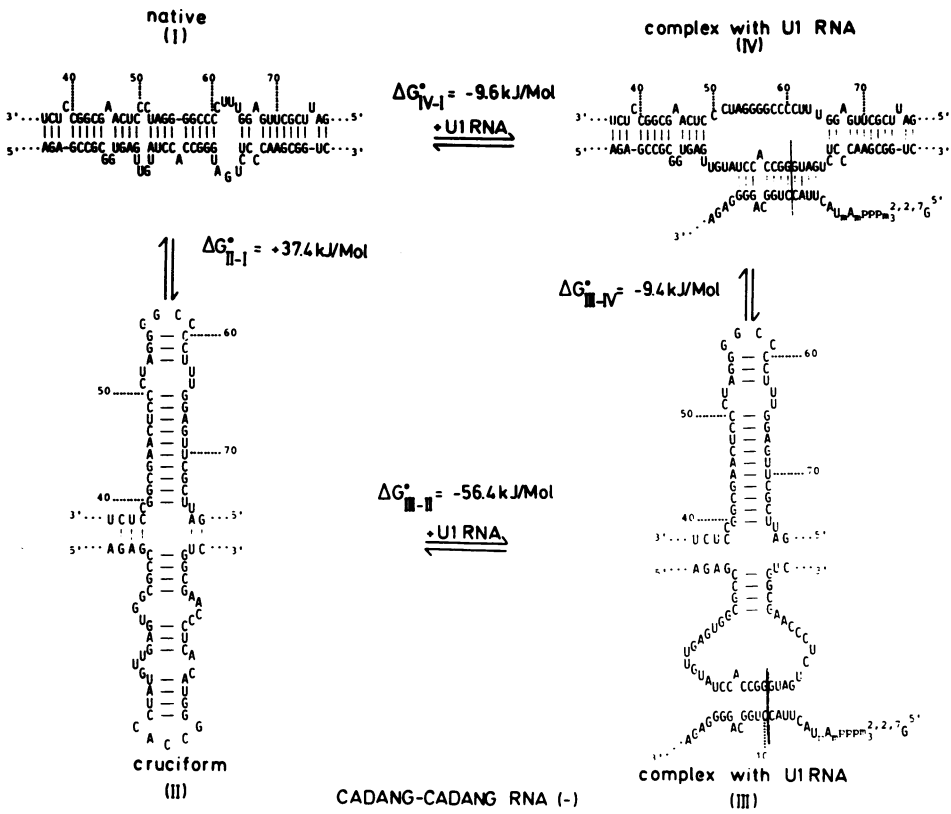

Fig. 8: Involvement of the stable hairpin in the splicing hypothesis. In the cruciform structure (II) the upper helical region is the stable hairpin which was found experimentally at higher temperature whereas the lower helical region is not stable under the same experimental conditions. ΔG°-values refer to 25°C, I M ionic strength. The vertical line is the hypothetical splicing site.

of it cannot be expected in ccRNA2. In accordance with this the main transition is less cooperative and at lower temerature.

4) The stable hairpin is possibly involved in splicing interference

It has recently been suggested that viroids may interfere with the splicing process or may have originated as escaped introns /16,34,35/. These hypotheses were based on the striking sequence homology between a segment of the viroids and a specific segment near the 5'end of U1RNA which is nearly identical in U1RNA from several different sources. According to Lerner et al. /36/ this segment in U1RNA may base pair with intron regions around the splicing site and serve as a structural prerequisite for the splicing process.

With a similar segment, viroids may be able to replace U1RNA thus leading to misregulation of splicing. The complementary copies of the viroid sequences, on the other hand, could bind directly to U1RNA.

The splicing interference hypothesis of viroids is of particular interest in this work because it is exactly the conservative sequence in ccRNA (i.e. the boxed in segment in Fig. 6) which is important in the hypothesis. Therefore, the hypothesis could also apply to ccRNA. Whereas the U1RNA-like sequence is in the lower part of the viroid strand, its opposite part in the upper strand carries the stable hairpin which has been characterized above. In Fig. 8 it is shown that quite different structures may occur if both, the splicing-interaction and the formation of the stable hairpin are considered. The complementary sequence of ccRNA is taken as an example because it is interacting with U1RNA and the same basepairs as in the literature can be assumed to be interacting in that example. ΔG-values have been estimated for the four transitions shown. It follows that the transitions from the native, extended form (I) to the cruciform (II) is highly improbable under physiological conditions. The probability changes drastically, however, if the U1RNA is interacting with the complement viroid. Now, the cruciform structure of the viroid is the more favorable structure. The functional relevance of the stable hairpin would then be to compete with the native structure and to make its opposite part in the viroid strand accessible for interaction with either U1RNA, or with the splicing site of heteronuclear RNA.

ACKNOWLEDGEMENTS

We thank Dr. Symons and Mr. Haseloff for making available for us the sequences prior to publication and reading critically the manuscript. Furthermore we wish to thank Dr. U. Rokohl for help in the computer work. The help of Mrs. H. Gruber in preparing the manuscript is acknowledged. The work was supported by grants from the Deutsche Forschungsgemeinschaft, Fonds der Chemischen Industrie, and Minister für Wissenschaft und Forschung des Landes Nordrhein-Westfalen. One of us (J.W.R.) was recipient of a Ludwig-Leichhardt commemorative fellowship of the Alexander von Humboldt-Stiftung.

*On leave from: Department of Plant Pathology, Waite Agricultural Research Institute, University of Adelaide, Glen Osmond, S.A. 5064, Australia

REFERENCES

1. Randles, J.W. (1975) Phytopathology, 65, 164-167.
2. Randles, J.W., Rillo, E.P., and Diener, T.O. (1976) Virology, 74, 128-139.

3. Diener, T.O. (1979) John Wiley and Sons. Inc., New York.
4. Randles, J.W., and Hatta, T. (1979) Virology, 96, 47-53.
5. ccRNA: RNA which is associated with the cadang-cadang-disease.
6. Randles, J.W., and Palukaitis, P. (1979) J. gen. Virol., 43, 649-662.
7. Imperial, J.S., Rodriguez, M.J.B., and Randles, J.W. (1982) J. gen. Virol. 56, 77-86.
8. Randles, J.W., Boccardo, G., Retuerma, M.L., and Rillo, E.P. (1971) Phytopathology, 67, 1211-1216.
9. VTMoV: Velvet tobacco mottle virus
SNMV: Solanum nodiflorum mottle virus.
10. Randles, J.W., Davies, C., Hatta, T., Gould, A.R., and Francki, R.I.B. (1981) Virology, 108, 111-122.
11. Gould, A.R. (1981) Virology, 108, 123-133.
12. Gould, A.R., and Hatta, T. (1981) Virology, 109, 137-147.
13. Gould, A.R., Francki, R.I.B., and Randles, J.W. (1981) Virology, 110, 420-426.
14. Gross, H.J., Domdey, H., Lossow, Ch., Jank, P., Raba, M., Alberty, H., and Sänger, H.L. (1978) Nature, 273, 203-208.
15. Haseloff, J., and Symons, R.H. (1981) Nucleic Acids Res., 9, 2741-2752.
16. Gross, H.J., Krupp, G., Domdey, H., Raba, M., Jank, P., Lossow, Ch., Alberty, H., Ramm, K., and Sänger, H.L. (1982) Eur. J. Biochem., 121, 249-257.
17. Riesner, D., Henco, K., Rokohl, U., Klotz, G., Kleinschmidt, A.K., Domdey, H., Jank, P., Gross, H.J., and Sänger, H.L. (1979) J. Mol. Biol., 133, 85-115.
18. Henco, K., Sänger, H.L., and Riesner, D. (1979) Nucleic Acids Res., 6, 3041-3060.
19. Haseloff, J., Mohamed, N.A., and Symons, R.H. (1982) Nature, in press.
20. Haseloff, J., and Symons, R.H. (1982)Nuclic Acids Res., 10,3681-3691.
21. Langowski, J., Henco, K., Riesner, D., and Sänger, H.L. (1978) Nucleic Acids Res., 5, 1589-1610.
22. Mohamed, N.A., Imperial, J.S., Buenaflor, G., and Rodriguez, J.B., manuscript in preparation.
23. Randles, J.W., Harrison, B.D., Mayo, M., and Murant, A.K. (1977) J. gen. Virol., 36, 187-193.
24. Ralph, R.K., and Bellamy, R. (1964) Biochim. Biophys, Acta., 87, 9-16.
25. Steger, G., Müller, H., and Riesner, D. (1980) Biochim. Biophys. Acta., 606, 274-284.
26. Henco, K., Steger, G., Riesner, D. (1980) Analyt. Biochem., 101, 225-229.
27. Fresco, J.R., Klotz, L.C., and Richards, E.G. (1963) Cold Spring Harb. Symp. Quant. Biol., 18, 83-90.
28. Coutts, S.M. (1971) Biochim. Biophys. Acta., 232, 94-106.
29. Coutts, S.M., Riesner, D., Römer, R., Rabl, C.R., and Maass, G. (1975) Biophys. Chem., 3, 275-289.
30. Riesner, D., Colpan, M., and Randles, J.W. (1982) Analyt. Biochem., 121, 186-189.
31. Pingoud, A., Boehme, D., Riesner, D., Kownatzki, R., and Maass, G. (1975) Eur. J. Biochem., 56, 617-622.
32. Riesner, D., Kaper, J., and Randles, J.W., accompanying paper.
33. Gross, H.J., Krupp, G., Domdey, H., Steger, G., Riesner, D., and Sänger, H.L. (1981) Nucleic Acids Res., Symposium Series, 10, 91-98.
34. Diener, T.O. (1981) Proc. Natl. Acad. Sci. USA, 78, 5014-5015.
35. Dickson, E. (1981) Virology, 115,, 216-221.
36. Lerner, M.R., Boyle, J.A., Mount, S.M., Wolin, S.L., and Steitz, J.A. (1980) Nature, 283, 220-224.